JACS
JOURNAL OF THE AMERICAN CHEMICAL SOCIETY

Article

pubs.acs.org/JACS

Construction of Ultrastable Porphyrin Zr Metal−Organic Frameworks through Linker Elimination

Dawei Feng, Wan-Chun Chung, Zhangwen Wei, Zhi-Yuan Gu, Hai-Long Jiang, Ying-Pin Chen, Donald J. Darensbourg, and Hong-Cai Zhou*

Department of Chemistry, Texas A&M University, College Station, Texas 77843, United States

Supporting Information

ABSTRACT: A series of highly stable MOFs with 3-D nanochannels, namely PCN-224 (no metal, Ni, Co, Fe), have been assembled with six-connected Zr_6 cluster and metalloporphyrins by a linker-elimination strategy. The PCN-224 series not only exhibits the highest BET surface area ($2600 m^2/g$) among all the reported porphyrinic MOFs but also remains intact in pH = 0 to pH = 11 aqueous solution. Remarkably, PCN-224(Co) exhibits high catalytic activity for the CO_2/propylene oxide coupling reaction and can be used as a recoverable heterogeneous catalyst.

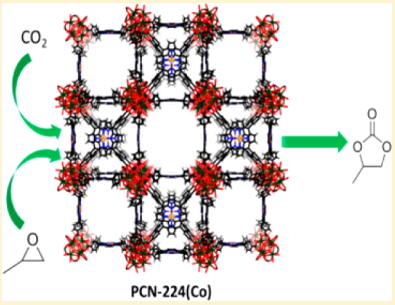

INTRODUCTION

Metal−organic frameworks (MOFs), an emerging class of organic−inorganic hybrid porous solids, have attracted a great deal of research interest for their potential applications, especially in gas storage and separation, catalysis, drug delivery, and sensing.[1,2] Moreover, the tunable nature of MOFs offers a unique advantage over other porous materials in that functional moieties can be readily introduced into the frameworks by either ligand design or postsynthetic modification.[3] Consequently, the incorporation of different functionalities into MOFs has been widely investigated toward various applications.[4]

Metalloporphyrins exhibit excellent catalytic activities. Immobilization of porphyrin catalysts in polymers and zeolites has been extensively explored. With uniform but tunable pore sizes, MOFs provide a special platform for the effective utilization of the porphyrinic catalytic centers. Recently, porphyrin derivatives have been introduced into MOFs by either linker extension or encapsulation.[5] Catalytic activities and optical properties have been investigated in such porphyrinic MOFs. However, most of these MOFs are constructed by the combination of soft acids (low-oxidative transition metal ions) and hard bases (carboxylates), and consequently have relatively weak chemical stabilities. Hence, the applications of porphyrinic MOFs in catalysis have been restricted to mild reaction conditions.

To improve the stability of porphyrinic MOFs and to facilitate the study of their catalytic activities, a chemically stable MOF is a prerequisite. So far, very few MOFs have high chemical stability, most of which are based on either high-oxidation-state metal species with carboxylate linkers or nitrogen containing ligands with divalent metals,[6] while Zr (IV)-based MOFs, an example of the former, are relatively less explored.[7] We are particularly interested in Zr-based MOFs because the strong interaction between Zr(IV) and carboxylate will make the resultant MOFs chemically stable; moreover, the modulating method makes Zr-MOF single crystals, suitable for structure determination, readily accessible.[8]

Combing the versatility of metalloporphyrins and the stability of Zr-carboxylate MOFs, we have reported an iron-porhpyrin zirconium MOF, PCN-222(Fe) (PCN stands for porous coordination network), which exhibits extraordinary stability and peroxidase-like catalytic activity.[9] In UiO-66, the Zr_6 cluster binds 12 carboxylates and exhibits O_h symmetry.[7a] Notably, in PCN-222, four of the surrounding carboxylate linkers connected to the Zr_6 cluster are replaced by hydroxyl groups. As a result, the O_h symmetry of the Zr_6 cluster is reduced to one of its subgroups, D_{4h}. The presence of fewer carboxylate linkers on the Zr_6 means more space for catalysis is available. Moreover, the introduction of OH groups improves the hardness of the Zr_6 core, which further strengthens the bonding between the bridging ligands and the Zr_6 units. Therefore, the PCN-222 series shows ultrahigh chemical stability. Such a linker-elimination strategy in the Zr_6 cluster inspires us to go further. By adjusting the reaction conditions, the coordination environment around the Zr_6 cluster could be tuned. MOFs containing novel Zr_6 clusters, which bind less than eight linkers with symmetry of another subgroup of O_h, could be obtained, which would allow us to construct new porphyrinic zirconium MOFs with new structures, high stability, and unexplored catalytic activity.

Bearing this in mind, by carefully varying the ratio of starting materials and the amount of modulating reagent, we have obtained a new series of porous porphyrinic zirconium MOFs, denoted PCN-224 based on a Zr_6 cluster with D_{3d} symmetry

Received: August 5, 2013
Published: October 14, 2013

ACS Publications © 2013 American Chemical Society

dx.doi.org/10.1021/ja408084j | J. Am. Chem. Soc. 2013, 135, 17105−17110

and MTCPP ligand (TCPP = tetrakis(4-carboxyphenyl)-porphyrin). PCN-224 possesses three-dimensional (3-D) channels as large as 19 Å and exhibits high stability over a wide range of pH in aqueous solution. Interestingly, PCN-224(Co) shows very high efficiency as a heterogeneous catalyst for the CO_2 and epoxide coupling reaction with good recyclability.

EXPERIMENTAL SECTION

Materials and Instrument. Methyl 4-formylbenzoate was purchased from Oakwood Products, Inc. Pyrrole, propionic acid, *N*,*N*-dimethylformamide (DMF), *N*,*N*-diethylformamide (DEF), benzoic acid, acetone, zirconium(IV) chloride, iron(II) chloride tetrahydrate ($FeCl_2{\cdot}4H_2O$), nickel(II) chloride hexahydrate ($NiCl_2{\cdot}6H_2O$), and cobalt(II) chloride hexahydrate ($CoCl_2{\cdot}6H_2O$) were purchased from Alfa Aesar. 5,10,15,20-Tetrakis(4-methoxycarbonylphenyl)porphyrin (TPPCOOMe) was prepared according to procedures described in Supporting Information section 2. All commercial chemicals were used without further purification unless otherwise mentioned.

Powder X-ray diffraction (PXRD) was carried out with a BRUKER D8-Focus Bragg–Brentano X-ray powder diffractometer equipped with a Cu sealed tube (λ = 1.541 78) at 40 kV and 40 mA. Elemental analyses (C, H, and N) were performed by Atlantic Microlab, Inc. (Norcross, Georgia). Thermogravimetric analyses (TGA) were conducted on a TGA-50 (SHIMADZU) thermogravimetric analyzer. Fourier transform infrared (IR) measurements were performed on a SHIMADZU IR Affinity-1 spectrometer. Gas sorption measurements were conducted using a Micrometritics ASAP 2420 system at various temperatures.

Synthesis of PCN-224(No Metal). $ZrCl_4$ (30 mg), H_2TCPP (10 mg), and 400 mg of benzoic acid in 2 mL of DMF were ultrasonically dissolved in a Pyrex vial. The mixture was heated in 120 °C oven for 24 h. After cooling down to room temperature, cubic dark purple crystals were harvested by filtration (10 mg, 71% yield). FTIR (KBr, cm^{-1}): 1664 (vs), 1601 (m), 1551 (m), 1497 (w), 1406 (vs), 1251 (m), 1179 (w), 1087 (s), 1022 (w), 974 (w), 808 (m), 772 (m), 728 (s), 662 (vs). Anal. Calcd (%) for PCN-224(no metal): C, 44.04; H, 2.62; N, 4.28%. Found: C, 50.34; H, 3.10; N, 3.64%.

Synthesis of PCN-224(Ni). $ZrCl_4$ (10 mg), Ni-TCPP (10 mg) and 250 mg of benzoic acid in 2 mL of DMF were ultrasonically dissolved in a Pyrex vial. The mixture was heated in 120 °C oven for 24 h. After cooling down to room temperature, dark red cubic crystals were harvested by filtration (10 mg, 70% yield). FTIR (KBr, cm^{-1}): 1661 (s), 1604 (m), 1548 (w), 1411 (vs), 1358 (s), 1254 (w), 1182 (w), 1108 (m), 998 (s), 802 (m), 772 (s), 716 (vs), 659 (vs). Anal. Calcd (%) for PCN-224(Ni): C, 42.22; H, 2.36; N, 4.10%. Found: C, 45.43; H, 3.13; N, 4.48%.

Synthesis of PCN-224(Co). $ZrCl_4$ (30 mg), CoTCPP (10 mg), and benzoic acid (400 mg) in 2 mL of DMF were ultrasonically dissolved in a Pyrex vial. The mixture was heated in 120 °C oven for 24 h. After cooling down to room temperature, dark red cubic crystals were harvested (10 mg, 70% yield). FTIR (KBr, cm^{-1}): 1664 (m), 1607 (m), 1548 (m), 1402 (vs), 1349 (m), 1212 (w), 1182 (w), 1096 (w), 995 (s), 835 (w), 799 (w), 772 (s), 713 (vs), 657 (vs). Anal. Calcd (%) for PCN-224(Co): C, 42.21; H, 2.36; N, 4.10%. Found: C, 46.74; H, 2.57; N, 3.73%.

Synthesis of PCN-224(Fe). $ZrCl_4$ (30 mg), FeTCPPCl (10 mg), and benzoic acid (400 mg) in 2 mL of DMF were ultrasonically dissolved in a 4 mL Pyrex vial. The mixture was heated in 120 °C oven for 12 h. After cooling down to room temperature, a mixture of dark brown square and needle shaped crystals (PCN-222) was harvested. Postsynthesis of pure phase PCN-224(Fe) follows: 200 mg of PCN-224(no metal) and 500 mg of $FeCl_2{\cdot}4H_2O$ were heated at 120 °C with stirring for 12 h. After that, the mixture was centrifuged. The liquid was decanted and the remaining solid washed with fresh DMF twice and acetone twice. The acetone was decanted, and the sample was dried in an oven. Brown crystals were obtained and demonstrated to be PCN-224 pure phase by PXRD. FTIR (KBr): ν = 3381 (m), 2952 (w), 1705 (w), 1601 (s), 1549 (s), 1411 (vs), 1340 (s), 1182 (m), 1003 (s), 871 (w), 809 (m), 776 (m), 723 (s) cm^{-1}. Anal. Calcd (%) for PCN-222(Fe): C, 42.12; H, 2.30; N, 4.08%. Found: C, 42.59; H, 3.12; N, 4.15%. Dark red cubic single crystals of PCN-224(Ni) and PCN-224(no metal) with suitable size for single-crystal X-ray diffraction have been obtained in our experiments. Other PCN-224 MOFs are confirmed by powder X-ray diffraction patterns.

Single-Crystal X-ray Crystallography. Single-crystal X-ray data of PCN-224(Ni) were collected on a Bruker Smart Apex diffractometer equipped with a low temperature device and a fine-focus sealed-tube X-ray source (Mo Kα radiation, λ = 0.710 73 Å, graphite monochromated). The data frames were collected using the program APEX2 and processed using the program SAINT routine within APEX2. The data were corrected for absorption and beam corrections based on the multiscan technique as implemented in SADABS. The structure was solved by direct methods and refined by full-matrix least-squares on F^2 with anisotropic displacement using the SHELXTL software package. Non-hydrogen atoms were refined with anisotropic displacement parameters during the final cycles. Hydrogen atoms on carbon and nitrogen were calculated in ideal positions with isotropic displacement parameters set to 1.2 × U_{eq} of the attached atoms, while hydroxide hydrogen atoms were not added into the structure. In the structure, free solvent molecules were highly disordered, and attempts to locate and refine the solvent peaks were unsuccessful. Contributions to scattering due to these solvent molecules were removed using the SQUEEZE routine of PLATON, and the structures were then refined again using the data generated. The contents of the solvent region are not represented in the unit cell contents in the crystal data. Crystallographic data and structural refinements for PCN-224(Ni) are summarized in Table S1 (Supporting Information).

Sample Activation and N_2 Adsorption Measuremnt. Before a gas sorption experiment, as-synthesized PCN-224 (~70 mg) samples were washed with DMF three times and once with acetone, and then immersed in acetone for over 12 h. After that, the mixture was centrifuged. After the removal of acetone by decanting, the samples were activated by drying under vacuum for 6 h, and then were dried again by using the "outgas" function of the adsorption instrument for 12 h at 80 °C prior to gas adsorption/desorption measurements.

Stability Test. A sample of 500 mg of freshly made PCN-224(Ni) was separated into 5 different vials containing 10 mL of 1 M HCl, pH = 1, pH = 10, pH = 11 aqueous solutions, and pure water. After immersion in those solutions for 24 h, PCN-224(Ni) samples were centrifuged and washed with acetone three times, and then dried on the vacuum line, and N_2 adsorption was measured on an ASAP 2420. The filtrate of each treatment was compared with 0.5 mg (1% of ligands containing in MOF sample) Ni-TCPP ligand aqueous solution.

Catalysis. PCN-224(Co) (45.7 mg, 0.0321 mmol), tetrabutylammonium chloride (19.9 mg, 0.0716 mmol), and propylene oxide (2.50 mL, 35.7 mmol) were added to a 12 mL autoclave reactor, which had previously been dried for 6 h. The reactor was pressurized to 2 MPa with CO_2 and maintained at 100 °C. After 4 h, the reactor was put into ice bath for 10 min and depressurized, and a small aliquot was taken to be analyzed by ^{1}H NMR to calculate the conversion of propylene oxide. The reaction solution was centrifuged to recover catalyst for the next cycle, and the supernatant was collected. The process was repeated using recovered catalyst, which had been dried in vacuo for 6 h.

RESULTS AND DISCUSSION

Single-crystal X-ray diffraction studies have revealed that PCN-224 crystallizes in space group $Im\bar{3}m$. Its framework consists of Zr_6 clusters linked by the square planar TCPP ligands. Each $Zr_6(OH)_8$ core, in which all of the triangular faces in a Zr_6-octahedron are capped by μ_3-OH groups (Figure 1c–e), is connected to six TCPP ligands.

Different from the 12-connected Zr_6 cluster observed in the UiO-66 and 8-connected Zr_6 cluster in PCN-222, only six edges

dx.doi.org/10.1021/ja408084j | J. Am. Chem. Soc. 2013, 135, 17105–17110

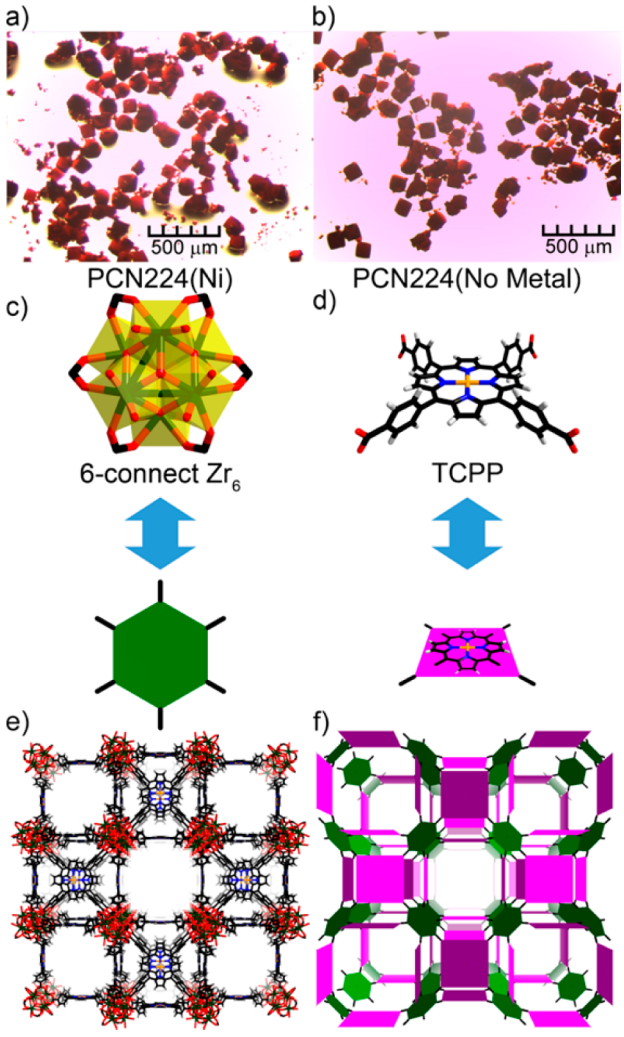

Figure 1. Microscope images of (a) PCN-224(Ni) and (b) PCN-224(no metal). Crystal structure, structural components, and underlying network topology of PCN-224(Ni): (c) the 6-connected D_{3d} symmetric Zr_6 in PCN-224. (d) Tetratopic TCPP ligands (violet square) with twisted dihedral angles generate a framework with 3-D nanochannels (e, f). Color scheme: Zr, green spheres; C, gray; O, red; N, blue; Ni, orange; and H, white.

of the Zr_6 octahedron are bridged by carboxylates from TCPP ligands in PCN-224. The lower connectivity on Zr_6 cluster is resulted from the increased Zr-TCPP ratio in the starting material. With triple the amount of Zr as in PCN-222, more Zr atoms would compete with each other to coordinate with TCPP ligand. Eventually, the connection numbers is eliminated to six, and the cluster symmetry is reduced to D_{3d} (Figure 2a).

Viewed along the S_6 axis, each triangle at the top and bottom of the Zr_6 octahedron is occupied by six terminal OH (or H_2O) groups (two on each Zr) giving rise to a D_{3d} symmetric Zr_6 cluster (Figure 1c). Moreover, the average dihedral angle between a phenyl ring and the porphyrin center of the ligand, 76.39°, is also different from that in PCN-222 (Figure 2b). With the reduced number of carboxylate linkers, the new Zr_6 cluster allows more free space, which eventually leads to the formation of 3-D channels. The solvent-accessible volume in PCN-224 reaches 78.9% calculated using the PLATON routine (1.8 Å probe).[10] As described above, the cluster and ligand can be viewed as 6- and 4-connected node, respectively. Thus, topologically, the framework can be classified as a 3-D (4,6)-

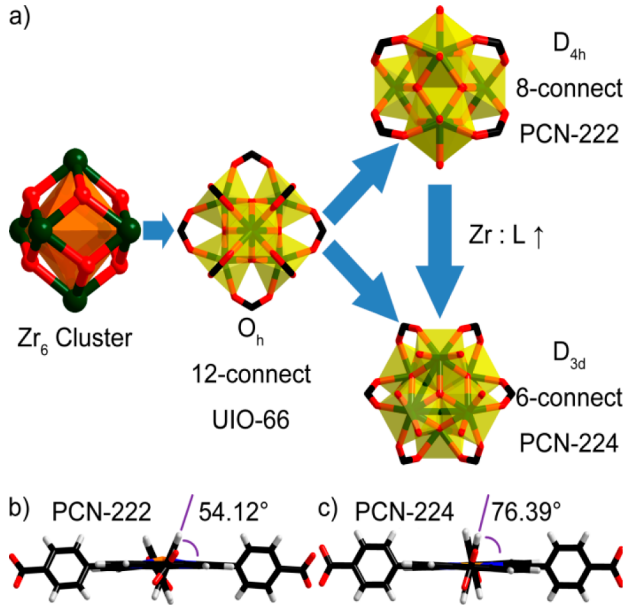

Figure 2. (a) Ligand elimination strategy in porphyrin zirconium MOFs. (b) Different dihedral angles between the porphyrin center and the benzene rings in TCPP ligand for PCN-222 and PCN-224.

connected **she** net with the point symbol $(4^4{\cdot}6^2)_3(4^6{\cdot}6^6{\cdot}8^3)_2$ (Figure 1f).

The porosity of PCN-224 series has been evaluated by nitrogen adsorption studies at 77 K. A N_2 uptake of 790 cm^3 g^{-1} (STP) and Brunauer–Emmett–Teller (BET) surface area of 2600 m^2 g^{-1} have been obtained for PCN-224(Ni). The N_2 adsorption shows a typical type-I isotherm, which is consistent with the crystal structure. The calculated total pore volume of PCN-224 is as high as 1.59 cm^3 g^{-1}. To the best of our knowledge, the BET surface area of PCN-224(Ni) represents the highest among all reported porphyrinic MOFs. Such high surface areas should be attributed to the 3-D large open channels in the framework, which makes most of the pore surface accessible. Other PCN-224 MOFs with different metal centers in the porphyrin also show similar N_2 adsorption isotherms and surface areas (Figure 3a,b).

With 3-D channels of 1.9 nm and lower connectivity on Zr_6 cluster, surprisingly, PCN-224 exhibits very high chemical stability. PCN-224 samples of the same batch were soaked in pH = 0 to pH = 11 aqueous solutions for 24 h. After that, those samples were centrifuged and reactivated. Powder X-ray diffraction (PXRD) patterns suggest that PCN-224 retains good crystallinity upon these treatments (Figure 4a). Such a wide range of pH stability is even better than our previously reported PCN-222. The N_2 adsorption isotherms of those samples show almost complete maintenance of the porosity, further demonstrating the framework stability (Figure 4b). Moreover, almost no dissolved ligand was detected in the filtrate after those chemical treatments (Figure 4c). Such good chemical stability has rarely been observed in other reported MOFs.

With 3-D open channels constructed from multifunctional porphyrin moieties, PCN-224(M) exhibits high chemical and thermal stability and meets most of the prerequisites as an ideal platform for heterogeneous catalysis.

First, with free porphyrin as the building block, PCN-224 allows the convenient insertion of various metals for different

dx.doi.org/10.1021/ja408084j | J. Am. Chem. Soc. 2013, 135, 17105–17110

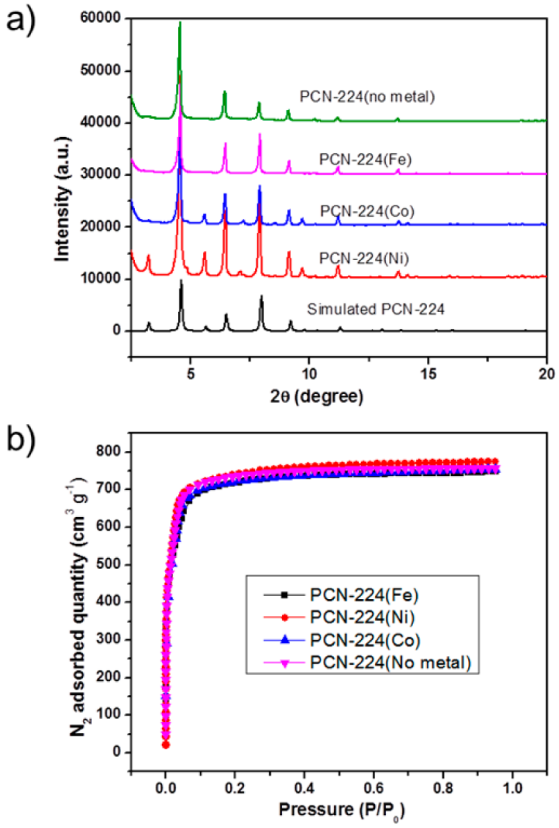

Figure 3. (a) Powder XRD patterns for simulated and experimental PCN-224 samples. (b) N_2 adsorption isotherm of PCN-224 series at 77 K, 1 atm.

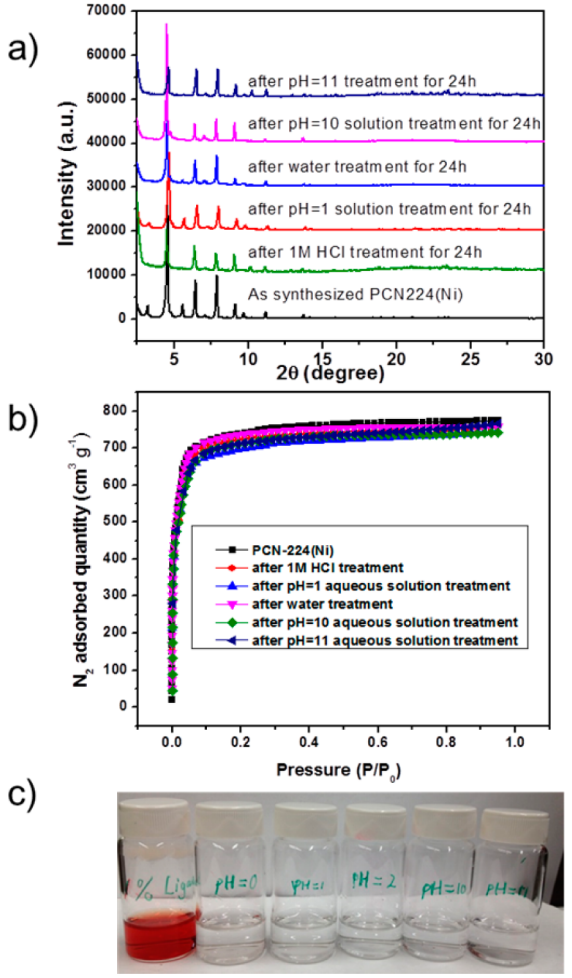

Figure 4. (a) PXRD patterns and (b) N_2 adsorption isotherms for PCN-224(Ni), showing the framework stability of PCN-224(Ni) upon treatments in 1 M HCl, pH = 1, water, and pH = 10 and pH = 11 aqueous solutions. (c) Comparison between 1 mg dissolved ligand and the corresponding solutions after the stability test.

types of catalysis and other applications under chemically harsh conditions.

Second, as an assembly of metalloporphyrins, PCN-224(M) provides evenly distributed catalytic centers, different from metalloporphyrins encapsulated in porous materials.

Third, the 3-D nanochannels allow fast diffusion and transportation of substrates and products. Therefore, the catalytic efficiency could be highly improved compared to MOFs with smaller pores.

Last, excellent stability, especially stability over a wide pH range, allows the application of PCN-224(M) as a reusable heterogeneous catalyst under harsh reaction conditions. With the most important advantage of heterogeneous catalysis, which is that it is easy to separate the catalyst from the reaction mixture, catalyst efficiency could be maintained and contamination from catalyst decomposition could be avoided.

Being a main cause of the greenhouse effect, CO_2 is also an abundant, cheap, and nontoxic renewable C1 resource. The development of efficient catalytic processes for CO_2 transformation into desirable, economically useful products is therefore of great interest. In particular, cyclic carbonates are an important class of compounds that can be used in various areas, such as polar aprotic solvents, degreasers, electrolytes in lithium ion batteries, as well as intermediates for linear dialkyl carbonate synthesis.[11]

Metalloporphyrins have been employed as catalysts in the presence of additives for the production of cyclic carbonates from CO_2 and epoxides.[12] For example, in early studies, Inoue and co-workers prepared propylene carbonate in modest yields over long reaction times from propylene oxide and CO_2 in the presence of an aluminum porphyrinate complex and *N*-methylimidazole.[13] Similarly, chromium(III) porphyrinate and DMAP have afforded cyclic carbonates from various epoxides/CO_2 with moderate TOFs at 70−100 °C (40−90 h^{-1}).[14] In studies related to those reported herein, Nguyen and co-workers have successfully utilized cobalt(III) porphyrin/DMAP catalyst systems for the synthesis of various cyclic carbonates from the corresponding epoxides and CO_2 under 17 atm pressure of CO_2 at 120 °C with TOFs varying widely with catalyst systems.[15] Jing and co-workers have extended these investigations to include tetraphenyl porphyrin with various cocatalysts, as well as other less effective metals such as manganese, iron, and ruthenium.[16] Hence, we have evaluated PCN-224(Co) as a heterogeneous catalyst for such a purpose (Figure 5a). In a typical reaction, PCN-224(Co) (32.1 μmol), tetrabutylammonium chloride (71.6 μmol), and propylene oxide (35.7 mmol) were added into an autoclave reactor. The reactor was pressurized to 2 MPa with CO_2 and maintained at 100 °C for 4 h. After that, PCN-224(Co) was recovered and reused in the next run under the same conditions. Even after three consecutive catalysis runs, the catalyst was demonstrated to be highly crystalline by PXRD (Figure 5b), which indicates the reusability of PCN-224(Co) as a heterogeneous catalyst.

dx.doi.org/10.1021/ja408084j | J. Am. Chem. Soc. 2013, 135, 17105−17110

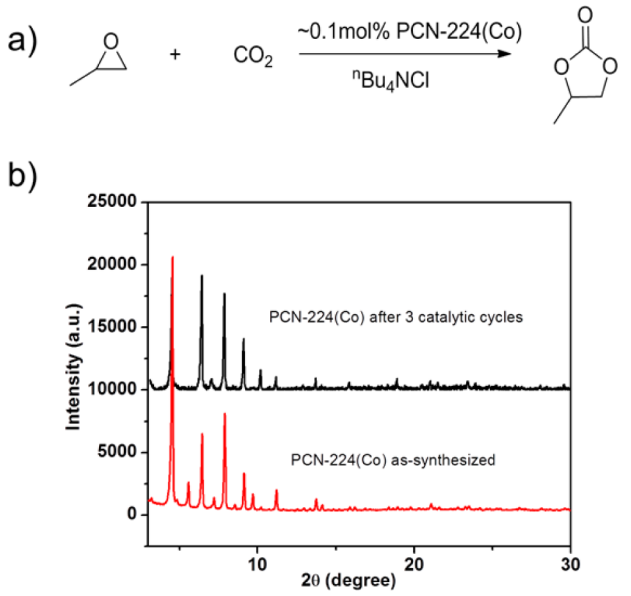

Figure 5. (a) CO_2 and propylene oxide coupling reaction catalyzed by PCN-224(Co) and (b) PXRD patterns of PCN-224(Co) as-synthesized sample (red) and after 3 catalytic cycles (black).

The resulting solution of each trial was analyzed by ^{1}H NMR to calculate the conversion of propylene oxide (Table 1).

Table 1. CO_2/Propylene Oxide Coupling Reaction Catalyzed by PCN-224(Co)

run	conversion (%)	TON[a]	TOF (h^{-1})[b]
1	42	461	115
2	33	419	104
3	39	518	129

[a]Moles of propylene oxide consumed/moles of Co. [b]Moles of propylene oxide consumed/moles of Co/reaction time.

Compared to the result from the homogeneous cobalt-porphyrin catalyst,[11a] PCN-224(Co) shows similar heterogeneous catalytic activity, which implies that the reaction is not under diffusion control, thanks to the 3-D nanochannels of PCN-224. Despite this interesting catalytic activity, the advantage of MOFs as heterogeneous catalysts can be further explored. For instance, normally the CO_2 pressure should remain high to make desirable portions dissolve in solution. However, with a MOF as a heterogeneous catalyst, the reaction can be conducted in the gas phase, in which CO_2 and epoxide gas can diffuse to the catalytic center more easily than in the liquid phase without any solubility concern. Moreover, with the gas phase starting materials, catalyzed by solid MOFs, generating liquid products, the separation process would be significantly simplified.

CONCLUSION

In conclusion, we have synthesized a series of new porphyrinic zirconium MOFs, PCN-224(M), by adopting a linker eliminations approach. The PCN-224(M) series exhibits high surface area and 3-D open channels. Moreover, PCN-224 shows remarkable stability in a wide range pH aqueous solution. In particular, PCN-224(Co) was demonstrated to be a reusable heterogeneous catalyst for the CO_2/epoxide coupling reaction.

ASSOCIATED CONTENT

Supporting Information

Full details for sample preparation and characterization results, and crystallographic data (CIF). This material is available free of charge via the Internet at http://pubs.acs.org.

AUTHOR INFORMATION

Corresponding Author

zhou@mail.chem.tamu.edu

Notes

The authors declare no competing financial interest.

ACKNOWLEDGMENTS

This work was supported as part of the Center for Gas Separations Relevant to Clean Energy Technologies, an Energy Frontier Research Center funded by the U.S. Department of Energy, Office of Science, Office of Basic Energy Sciences under Award Number DE-SC0001015.

REFERENCES

(1) Zhou, H.-C.; Long, J. R.; Yaghi, O. M. *Chem. Rev.* **2012**, *112*, 673.
(2) (a) Jiang, H.-L.; Xu, Q. *Chem. Commun.* **2011**, *47*, 3351. (b) Gu, Z.-Y.; Yang, C.-X.; Chang, N.; Yan, X.-P. *Acc. Chem. Res.* **2012**, *45*, 734. (c) Farrusseng, D.; Aguado, S.; Pinel, C. *Angew. Chem., Int. Ed.* **2009**, *48*, 7502. (d) Corma, A.; García, H.; Llabrés i Xamena, F. X. *Chem. Rev.* **2010**, *110*, 4606.
(3) Cohen, S. M. *Chem. Rev.* **2012**, *112*, 970.
(4) (a) Horcajada, P.; Gref, R.; Baati, T.; Allan, P. K.; Maurin, G.; Couvreur, P.; Férey, G.; Morris, R. E.; Serre, C. *Chem. Rev.* **2012**, *112*, 1232. (b) Kreno, L. E.; Leong, K.; Farha, O. K.; Allendorf, M.; Van Duyne, R. P.; Hupp, J. T. *Chem. Rev.* **2012**, *112*, 1105. (c) Suh, M. P.; Park, H. J.; Prasad, T. K.; Lim, D.-W. *Chem. Rev.* **2012**, *112*, 782. (d) Sumida, K.; Rogow, D. L.; Mason, J. A.; McDonald, T. M.; Bloch, E. D.; Herm, Z. R.; Bae, T.-H.; Long, J. R. *Chem. Rev.* **2012**, *112*, 724-. (e) Yoon, M.; Srirambalaji, R.; Kim, K. *Chem. Rev.* **2012**, *112*, 1196. (f) Cui, Y.; Yue, Y.; Qian, G.; Chen, B. *Chem. Rev.* **2012**, *112*, 1126. (g) Li, J.-R.; Sculley, J.; Zhou, H.-C. *Chem. Rev.* **2012**, *112*, 869. (h) Wu, H.; Gong, Q.; Olson, D. H.; Li, J. *Chem. Rev.* **2012**, *112*, 836. (i) Wang, C.; Zhang, T.; Lin, W. *Chem. Rev.* **2012**, *112*, 1084−1104. (j) Lu, W.-G.; Su, C.-Y.; Lu, T.-B.; Jiang, L.; Chen, J.-M. *J. Am. Chem. Soc.* **2005**, *128*, 34. (k) Umemura, A.; Diring, S.; Furukawa, S.; Uehara, H.; Tsuruoka, T.; Kitagawa, S. *J. Am. Chem. Soc.* **2011**, *133*, 15506.
(5) (a) Alkordi, M. H.; Liu, Y.; Larsen, R. W.; Eubank, J. F.; Eddaoudi, M. *J. Am. Chem. Soc.* **2008**, *130*, 12639. (b) Fateeva, A.; Chater, P. A.; Ireland, C. P.; Tahir, A. A.; Khimyak, Y. Z.; Wiper, P. V.; Darwent, J. R.; Rosseinsky, M. J. *Angew. Chem., Int. Ed.* **2012**, *51*, 7440. (c) Meng, L.; Cheng, Q.; Kim, C.; Gao, W.-Y.; Wojtas, L.; Chen, Y.-S.; Zaworotko, M. J.; Zhang, X. P.; Ma, S. *Angew. Chem., Int. Ed.* **2012**, *51*, 10082. (d) Morris, W.; Volosskiy, B.; Demir, S.; Gándara, F.; McGrier, P. L.; Furukawa, H.; Cascio, D.; Stoddart, J. F.; Yaghi, O. M. *Inorg. Chem.* **2012**, *51*, 6443. (e) Son, H.-J.; Jin, S.; Patwardhan, S.; Wezenberg, S. J.; Jeong, N. C.; So, M.; Wilmer, C. E.; Sarjeant, A. A.; Schatz, G. C.; Snurr, R. Q.; Farha, O. K.; Wiederrecht, G. P.; Hupp, J. T. *J. Am. Chem. Soc.* **2013**, *135*, 862. (f) Zou, C.; Xie, M.-H.; Kong, G.-Q.; Wu, C.-D. *CrystEngComm* **2012**, *14*, 4850.
(6) (a) Férey, G.; Mellot-Draznieks, C.; Serre, C.; Millange, F.; Dutour, J.; Surblé, S.; Margiolaki, I. *Science* **2005**, *309*, 2040. (b) Férey, G.; Serre, C.; Mellot-Draznieks, C.; Millange, F.; Surblé, S.; Dutour, J.; Margiolaki, I. *Angew. Chem., Int. Ed.* **2004**, *43*, 6296. (c) Guillerm, V.; Ragon, F.; Dan-Hardi, M.; Devic, T.; Vishnuvarthan, M.; Campo, B.; Vimont, A.; Clet, G.; Yang, Q.; Maurin, G.; Férey, G.; Vittadini, A.; Gross, S.; Serre, C. *Angew. Chem., Int. Ed.* **2012**, *51*, 9267. (d) Kandiah, M.; Nilsen, M. H.; Usseglio, S.; Jakobsen, S.; Olsbye, U.; Tilset, M.; Larabi, C.; Quadrelli, E. A.; Bonino, F.; Lillerud, K. P. *Chem. Mater.* **2010**, *22*, 6632. (e) Banerjee, R.; Phan, A.; Wang, B.; Knobler, C.; Furukawa, H.; O'Keeffe, M.; Yaghi, O. M. *Science* **2008**, *319*, 939.

(f) Hayashi, H.; Cote, A. P.; Furukawa, H.; O'Keeffe, M.; Yaghi, O. M. *Nat. Mater.* **2007**, *6*, 501. (g) McDonald, T. M.; D'Alessandro, D. M.; Krishna, R.; Long, J. R. *Chem. Sci.* **2011**, *2*, 2022. (h) Wang, B.; Cote, A. P.; Furukawa, H.; O'Keeffe, M.; Yaghi, O. M. *Nature* **2008**, *453*, 207.

(7) (a) Cavka, J. H.; Jakobsen, S.; Olsbye, U.; Guillou, N.; Lamberti, C.; Bordiga, S.; Lillerud, K. P. *J. Am. Chem. Soc.* **2008**, *130*, 13850. (b) Wang, C.; Wang, J.-L.; Lin, W. *J. Am. Chem. Soc.* **2012**, *134*, 19895. (c) Wang, C.; Xie, Z.; deKrafft, K. E.; Lin, W. *J. Am. Chem. Soc.* **2011**, *133*, 13445. (d) Jiang, H.-L.; Feng, D.; Li, J.-R.; Liu, T.-F.; Zhou, H.-C. *J. Am. Chem. Soc.* **2012**, *134*, 14690.

(8) Schaate, A.; Roy, P.; Godt, A.; Lippke, J.; Waltz, F.; Wiebcke, M.; Behrens, P. *Chem.—Eur. J.* **2011**, *17*, 6643.

(9) Feng, D.; Gu, Z. Y.; Li, J. R.; Jiang, H. L.; Wei, Z.; Zhou, H. C. *Angew. Chem., Int. Ed.* **2012**, *51*, 10307.

(10) Spek, A. L. *J. Appl. Crystallogr.* **2003**, *36*, 7.

(11) (a) Paddock, R. L.; Hiyama, Y.; McKay, J. M.; Nguyen, S. T. *Tetrahedron Lett.* **2004**, *45*, 2023. (b) Lu, X.-B.; Darensbourg, D. J. *Chem. Soc. Rev.* **2012**, *41*, 1462.

(12) For comprehensive reviews in this area, see: (a) North, M.; Pasquale, R.; Young, C. *Green Chem.* **2010**, *12*, 1514−1539. (b) Lu, X.-B.; Darensbourg, D. J. *Chem. Soc. Rev.* **2012**, *41*, 1462.

(13) Takeda, N.; Inoue, S. *Bull. Chem. Soc. Jpn.* **1978**, *51*, 3564−3567.

(14) Kruper, W. J.; Dellar, D. V. *J. Org. Chem.* **1995**, *60*, 725−727.

(15) Paddock, R. L.; Hiyama, Y.; McKay, J. M.; Nguyen, S. T. *Tetrahedron Lett.* **2004**, *45*, 2023−2026.

(16) Jin, L.; Jing, H.; Chang, T.; Bu, X.; Wang, L.; Liu, Z. *J. Mol. Catal. A: Chem.* **2007**, *261*, 262−266.